Iranian Journal of Hydrogen & Fuel Cell 9(2022) 117-132

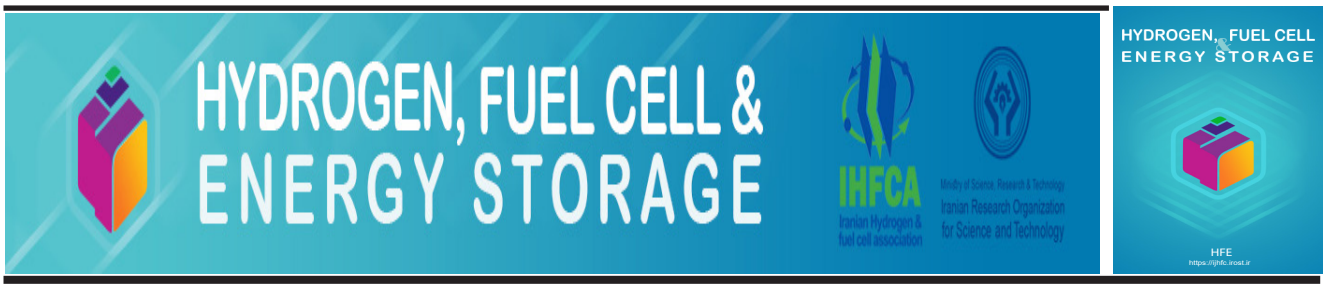

High Step-Up Converter with Low Voltage Stress for Fuel Cell Applications

Hossein Bagherian Farahabadi[1,*], Mostafa Kojoury-Naftchali[2], Amirhossein Pahnabi[3]

[1,3] Northern Research Center for Science & Technology, Malek Ashtar University of Technology, Iran
[2] Faculty of Electrical Engineering, Shahid Beheshti University, Tehran 1983969411, Iran

Article Information

Article History:

Received:
24 Sep 2022
Received in revised form:
10 Oct 2022
Accepted:
11 Oct 2022

Keywords

high step-up
DC-DC converter
fuel cell
switched capacitor-switched inductor
low voltage stress

Abstract

High step-up DC-DC converters are considered the main components of some low-voltage and low-power fuel cell power system applications. A new DC-DC converter topology based on a two-stage switched capacitor-switched inductor multiplier is proposed in this paper. In comparison with other conventional and high step-up DC-DC converters, the proposed converter topology provides higher voltage gain and lower switch voltage stresses for duty cycles in the range of 0.6 or higher, the typical duty cycle of high step-up DC-DC converters. The proposed converter consists of a novel combination of switched capacitors and switched inductors methods that reduce the number of required switches and their duty cycles. The theoretical analysis was confirmed by simulation results in MATLAB/Simulink software environment results. A 100 W laboratory prototype of the proposed converter was implemented to investigate and validate the analytical and simulation results. The prototype DC-DC converter was designed and implemented for use in a commercial 100 W PEM fuel cell stack power system.

1. Introduction

Long-term use of fossil fuels has caused many problems, such as environmental pollution, global warming, and the elimination of such energies. These outcomes emphasize the importance of using renewable energy sources [1-7]. In contrast to fossil fuels, renewable energies are not easy to use and usually need some power interface utilities. The utilities convert renewable energies into electrical energy, which can then be used for desired goals [3], [8,9]. The low output voltage of some renewable energy sources, such as low-voltage fuel cells, can be increased by utiliz-

*Corresponding Author: bagherian@mut.ac.ir

doi: 10.22104/IJHFC.2022.5869.1247

ing high gain DC-DC converters. A high gain DC-DC converter provides proper voltage levels with a specific conversion ratio, depending on the fuel cell voltage and load specifications [10-16]. Figure 1 shows the schematic structure of a fuel cell operating system containing a high gain DC-DC converter.

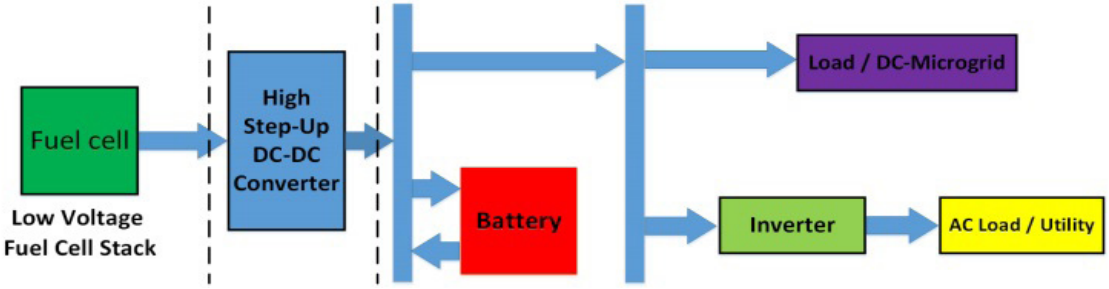

Fig. 1. Typical renewable energy system.

Due to limitations in voltage gain increment, conventional DC-DC boost converters are not appropriate in low-voltage fuel cells. Voltage gain increment in conventional DC-DC boost converters is accompanied by challenges such as excessive increasing of duty cycle, difficult pulse modulation performance, voltage spikes, and so on [17-20]. Therefore, using a high gain DC-DC converter is a better choice than the conventional DC-DC boost converter because of its higher quality and capability. There are conventional methods to achieve a high gain converter, such as the switched capacitor technique, coupled inductor technique, and interleaved technique. Each method has advantages and disadvantages, and the appropriate method should be selected based on the user's requirements. For example, using the switched capacitor technique to achieve high voltage gain forces the designer to use more switches in the converter structure, resulting in circuit complexity. On the other hand, using the coupled inductor technique leads to more expenses and weight. A good combination of these methods would be able to optimize their merits while preventing their defects.

In this paper, a novel topology for a high gain DC-DC converter for use in a fuel cell power system is proposed, and a laboratory prototype of the proposed converter is implemented. The proposed converter is able to provide desired operating conditions with low on-mode resistance, low conduction mode losses, and low switch voltage stress, leading to a more efficient steady-state performance [21-24]. The voltage multiplier in the proposed converter consists of a novel combination of switched capacitors and switched inductors methods to decrease the number of required switches and their duty cycles [25]. The multiplier of the proposed converter lowers the switch voltage spikes compared to other high step-up and conventional boost converters

The proposed converter is described theoretically, and specific parameters such as the converter, voltage gain, and voltage stress of its elements are analysed. Then the proposed converter simulation results in the MATLAB/Simulink software environment are presented and analysed. Finally, the experimental results for the proposed converter's 100 W laboratory prototype are presented to validate the theoretical and simulation results. The prototype high step-up converter was designed and implemented for use in a fuel cell power system with a Horizon H-100 fuel cell stack.

2. Operation principle of the proposed converter

The proposed converter topology is presented in Figure 2. As shown in Figure 2, the proposed converter

includes four sections: a typical boost converter, the first and second multiplier modules (combining the two multiplier modules form the multiplier section), and the output filter. The sections are connected in series.

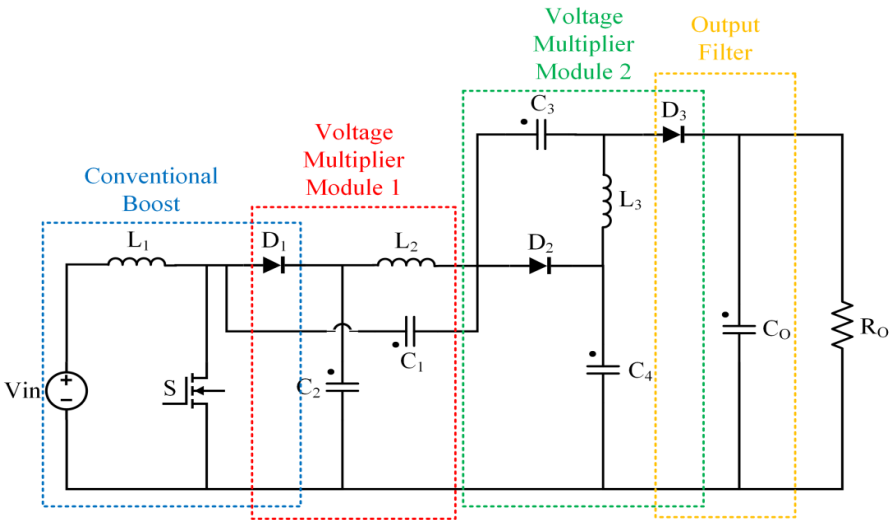

Fig. 2. Different sections of the proposed converter.

As shown in Figure 2, the proposed converter includes a MOSFET as switch S; three inductors L_1, L_2, and L_3; three diodes D_1, D_2, D_3; and five capacitors C_1, C_2, C_3, C_4, and C_O.

The following assumptions were made for the detailed analysis of the proposed converter:

(1) The proposed converter operates in continuous conduction mode (CCM).

(2) The capacitors are large enough, and their voltages can be assumed to be constant.

(3) The semiconductor devices are considered ideal, and their internal resistances are not considered.

The converter has four operation modes and consists of one switch and two multipliers that operate in continuous mode. The converter's equivalent circuits and waveforms are shown in Figures 3 and 4, respectively. Figure 4 includes the following waveforms: the MOSFET's gate-to-source voltage (V_{GS}) and drain-to-source voltage (V_{DS}), the input current (I_{in}) and voltage (V_{in}), the inductors L_1, L_2, and L_3 currents (I_{L1}, I_{L2}, and I_{L3}, respectively) and voltages (V_{L1}, V_{L2}, and V_{L3}, respectively), the diodes D_1, D_2 and D_3 currents (I_{D1}, I_{D2}, and I_{D3}, respectively) and voltages (V_{D1}, V_{D2}, and V_{D3}, respectively) and currents (I_{D1}, I_{D2}, and I_{D3}, respectively), and the capacitors C_1, C_2, C_3, C_4, and C_O (V_{C1}, V_{C2}, V_{C3}, V_{C4}, and V_{CO}, respectively).

3. Steady-state analysis of the proposed converter

In this section, the theoretical equations are derived for the proposed converter according to the assumptions given in section 2. Since the time integral of the inductor's voltage over one time period must be zero in a steady state, the volt-second equations are obtained for inductors L_1, L_2, and L_3. When the switch is on, inductors' voltages are obtained as (1)-(3):

$$V_{L1} = V_{in} \quad (1)$$

$$V_{L2} = V_{C2} - V_{C1} \quad (2)$$

$$V_{L3} = V_{C4} - V_{C1} - V_{C3} \quad (3)$$

When the switch is off, inductors' voltages are obtained as (4)-(6):

$$V_{L1} = V_{in} - V_{C2} \quad (4)$$

$$V_{L2} = V_{in} - V_{L1} - V_{C1} - V_{C2} = V_{C2} - V_{C4} \quad (5)$$

$$V_{L3} = V_{C4} - V_O \quad (6)$$

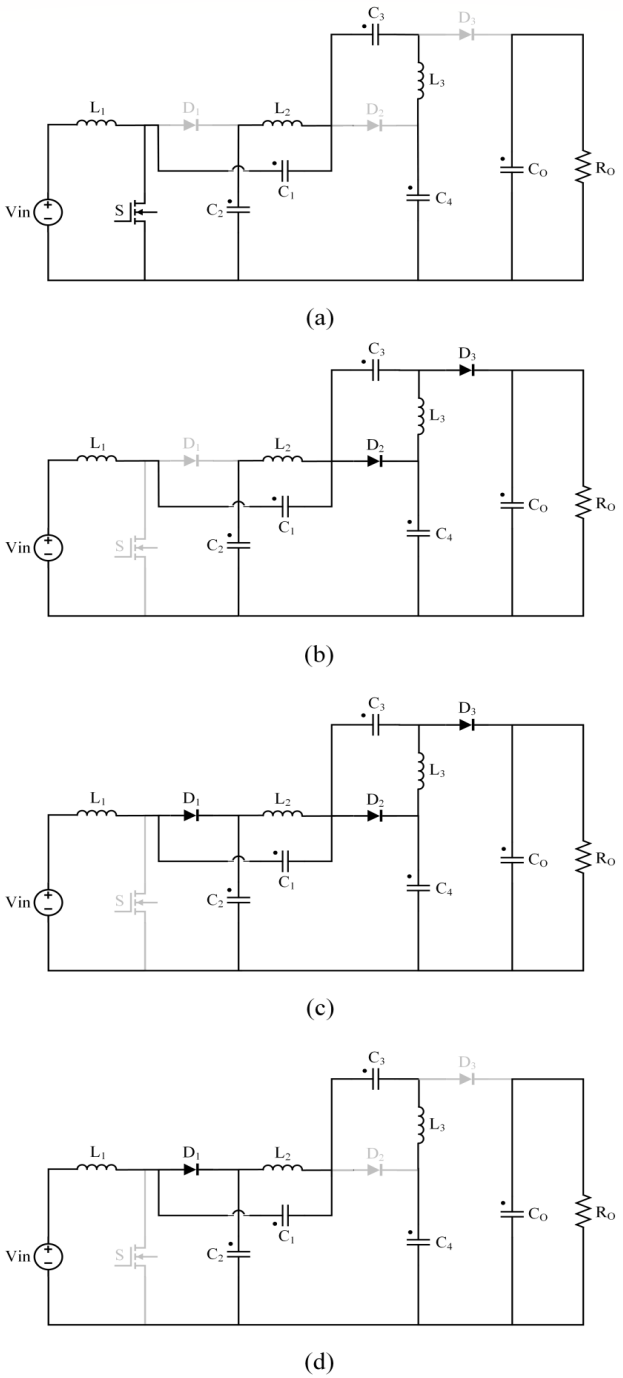

Fig. 3. Equivalent circuits of the proposed converter in different modes.

By using the volt-second balance for the inductor's L_1, L_2, and L_3, the following equations are obtained:

$$\int_0^{DT} V_{in}\,dt + \int_{DT}^{T} (V_{in} - V_{C2})\,dt = 0 \quad (7)$$

$$\int_0^{DT} (V_{C2} - V_{C1})\,dt + \int_{DT}^{T} (V_{in} - V_{L1} - V_{C1} - V_{C2})\,dt = 0 \quad (8)$$

$$\int_0^{DT} (V_{C4} - V_{C1} - V_{C3})\,dt + \int_{DT}^{T} (V_{C4} - V_O)\,dt = 0 \quad (9)$$

By simplifying equation (9) for the capacitor's voltage, the following equations are obtained:

$$V_{C1} = DV_{C2} \quad (10)$$

$$V_{C2} = \frac{V_{in}}{1-D} \quad (11)$$

$$V_{C3} = DV_{C2} \quad (12)$$

$$V_{C4} = (1+D)V_{C2} \quad (13)$$

Considering Figure 3-b, by applying KVL to the C_3, C_4, and C_o capacitors' voltages in the second mode of the converter operation, the following equation is derived:

$$V_O = V_{C3} + V_{C4} \quad (14)$$

Therefore, the converter voltage gain can be calculated as follows: (15)

$$V_O = V_{C3} + V_{C4} = DV_{C4} + V_{C4} = \frac{1+2D+D^2}{(1-D)} V_{in}, M = \frac{V_O}{V_{in}} = \frac{(1+D)^2}{(1-D)}$$

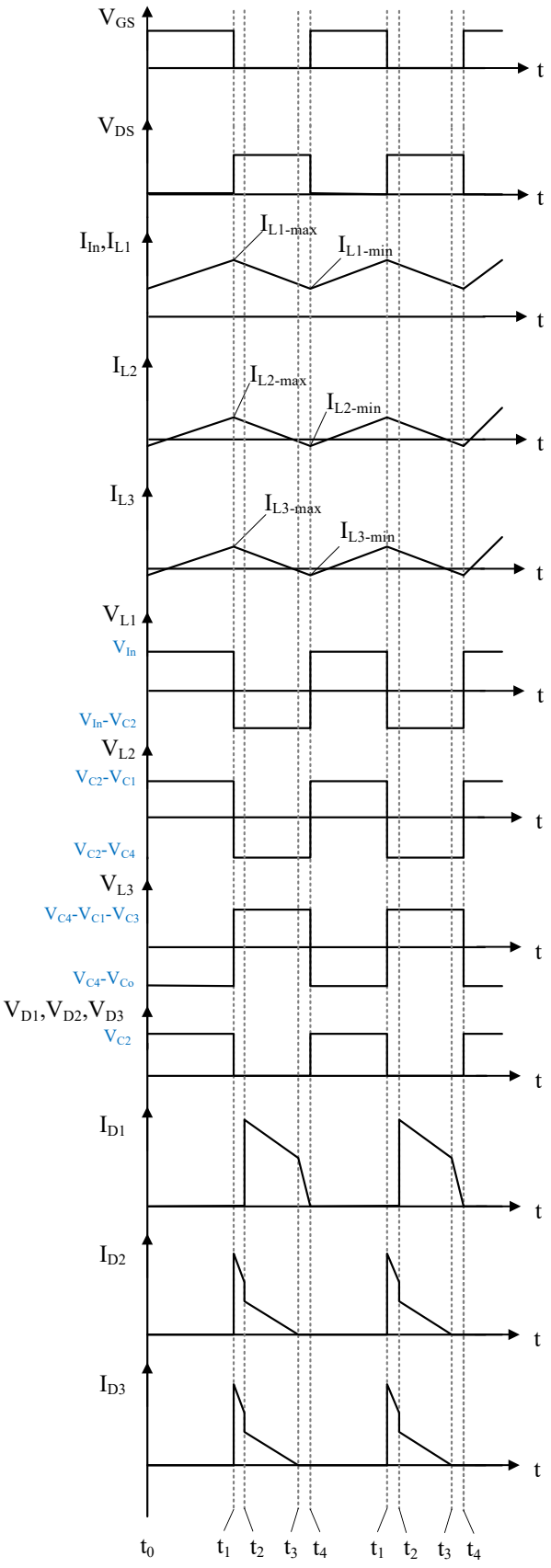

Fig. 4. Main waveforms of the proposed converter.

4. Voltage and current stress analysis

The voltage applied to the switch can be calculated as follows:

$$V_{DS} = V_{C2} = \frac{V_{in}}{(1-D)} \tag{16}$$

The voltage applied to diodes D1, D2, and D3 in the off-state can be described as:

$$V_{D1} = V_{C2} = \frac{V_{in}}{(1-D)} = \frac{V_O}{(1+D)^2} \tag{17}$$

$$V_{D2} = V_{C4} - V_{C1} = \frac{V_{in}}{(1-D)} = \frac{V_O}{(1+D)^2} \tag{18}$$

$$V_{D3} = V_O - V_{C1} - V_{C3} = \frac{V_{in}}{(1-D)} = \frac{V_O}{(1+D)^2} \tag{19}$$

According to equations (17) to (19), the voltages applied to the reverse-biased diodes are less than the output voltage. This is desirable because the semiconductors' voltage ratings do not exceed the converter's nominal output voltage.

The inductor and diode currents should be obtained to calculate the current stress. The capacitors' currents are neglected for simplicity and because the average current passing through the capacitors is zero. The inductors and diodes' currents are described as follows:

$$I_{L2} = I_{L3} = I_{D1} = I_{D2} = I_{D3} = I_O \tag{20}$$

Neglecting the power losses in the circuit, the input current, which is equal to the inductor L_1 current, can be calculated as follows:

$$I_{L1} = I_{in} = I_O.M = \frac{(1+D)^2}{(1-D)^2}.I_O \tag{21}$$

Considering Figure 3, the switch current in the first mode of the converter operation can be described as:

$$I_S = (I_{L1} - I_{L2}).D = M.I_O - I_O = \frac{3D}{(1-D)}.I_O \quad (22)$$

5. Comparison and evaluation

In this section, the proposed converter performance is compared and evaluated. Table 1 presents a brief comparison of the proposed converter and several conventional and high step-up converters.

Table1 . Performance Comparison of DC-DC Converters

Converter	Voltage Gain	Number of Switches	Number of Diodes	Switch Drain-Source Voltage	Diodes' Voltage Stress
Conventional boost	$\frac{1}{1-D}$	1	1	V_O	V_O
Reference [2]	$\frac{1+D}{1-D}$	1	2	$\frac{V_O}{1+D}$	$\frac{V_O}{1+D}$
Reference [3]	$\frac{1+2D}{1-D}$	1	4	V_O	V_O
Reference [7]	$\frac{3-D}{1-D}$	1	5	$\frac{V_O}{3-D}$	$\frac{1-D}{D(3-D)}V_O$
Reference [11]	$\frac{1}{D(1-D)}$	2	2	V_O	V_O
Reference [20]	$\frac{3-D}{1-D}$	1	4	$\frac{V_O}{3-D}$	$\frac{V_O}{3-D}$
Reference [21]	$\frac{2}{1-D}$	1	2	V_O	$\frac{V_O}{2}$
Proposed Converter	$\frac{(1+D)^2}{1-D}$	1	3	$\frac{V_O}{(1+D)^2}$	$\frac{V_O}{(1+D)^2}$

The voltage conversion ratio comparison between the proposed converter and the other converter topologies is shown in Figure 5. As can be seen, the proposed converter obtains a higher voltage gain for switch duty cycles above 0.57.

The normalized voltage stress across the switch's drain-source voltage is compared in Figure 6. As can be seen, as the duty cycle increases, the normalized voltage stress decrease rate is higher in the proposed converter. Also, for the cases in which the duty cycle is more than 0.62, the proposed converter has the lowest normalized switch voltage stress compared to the other converters. Therefore, considering the typical duty cycles for the high step-up DC-DC converters (usually 0.6 or higher), the proposed converter provides better performance than the other converter topologies.

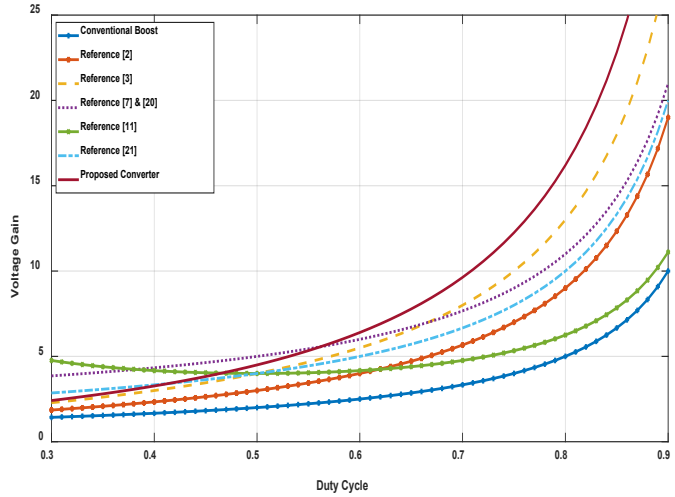

Fig. 5. Voltage gain comparison.

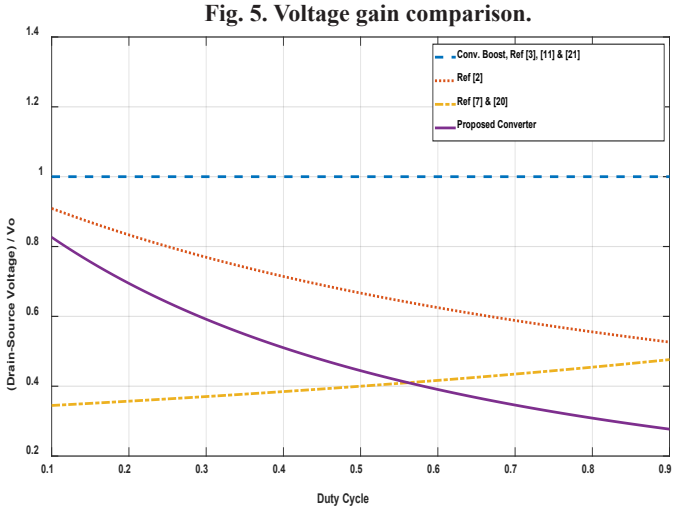

Fig. 6. Normalized voltage stress across the switch.

6. Design considerations of the proposed converter

As the converter is assumed to operate in the continuous conduction mode, the following equations can be written for the inductors:

$$L_1 = \frac{DV_{in}}{\Delta I_{L1} f_s} \tag{23}$$

$$L_2 = \frac{DV_{L2}}{\Delta I_{L2} f_s} = \frac{DV_{in}}{(1-D)\Delta I_{L2} f_s} \tag{24}$$

$$L_3 = \frac{DV_{L3}}{\Delta I_{L3} f_s} = \frac{D^2 V_{in}}{(1-D)\Delta I_{L3} f_s} \tag{25}$$

And for the capacitors:

$$C_1 = \frac{(1-D)I_{L1}}{f_s \Delta V_{C1}} \tag{26}$$

$$C_2 = \frac{(1-D)I_{L2}}{f_s \Delta V_{C2}} \tag{27}$$

$$C_3 = C_4 = \frac{DI_{L3}}{f_s \Delta V_{C3}} \tag{28}$$

$$C_O = \frac{(1-D)I_O}{f_s \Delta V_O} \tag{29}$$

Deriving the voltages and currents of the semiconductor switches and diodes is very important in the power electronic converters design process. The drain-source voltage applied to the switch for the proposed converter is derived in equation (16), and the switch current is derived in equation (22). The diodes' voltages are derived in equations (17-19), and the diodes' currents can be calculated from equation (20). However, some environmental and parasitic effects in the converter practical tests may disrupt the desired converter performance. Therefore, some certainty margins should be considered in the circuit elements selection process [26].

7. Simulation

As mentioned previously, the prototype converter is designed and implemented to be used for a fuel cell power system with a Horizon H-100 fuel cell stack. The performance characteristics of the stack, including the voltage-current and power-current curves, are presented in Figure 7.

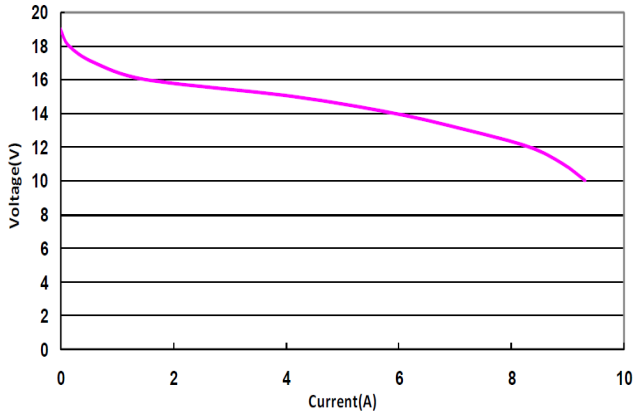

(a)

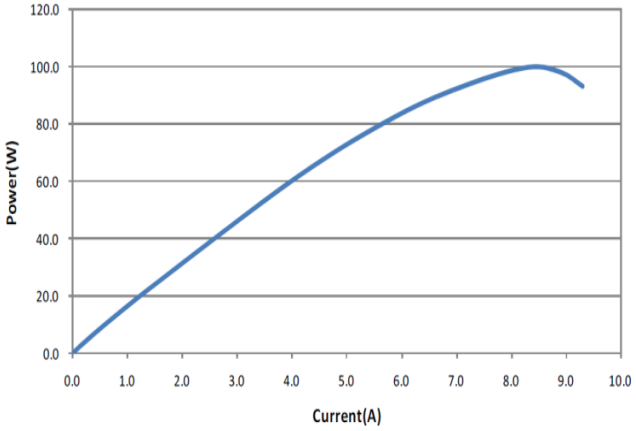

(b)

Fig. 7. Performance characteristics of the stack including a) voltage-current curve and b) power-current curve [27].

The converter loading level is specified in such a way that the operating voltage point of the stack becomes about 12 V, and as can be seen in Figure 7-b, the stack power, which is equal to the converter input power, is about 100 W. The switching frequency and the duty cycle selected are 32 kHz and 63%, respectively. Therefore the circuit elements' values are determined by equations (23) to (29).

The proposed converter was simulated in the MATLAB/Simulink software environment to verify the analytical results. The quantities derived from the analytical equations are slightly modified to improve the converter performance at the fuel cell stack operating point and use capacitors with standard values. The inductors' and capacitors' values are given in Table 2.

Table2 . The Values of Inductors and Capacitors of the Proposed Converter

Component	Value
L_1, L_2, L_3	50 µH
C_1, C_2, C_3, C_4	33 µF
C_O	56 µF

The drain-source voltage and current waveforms of the switch are shown in Figure 8. The inductors' currents are shown in Figure 9. As can be seen in Figure 9-a, the converter operates in the continuous conduction mode.

The diodes' reversed voltages and currents are shown in Figure 10. As seen in the figure, the peak value of the diodes' reverse voltages is almost less than half of the output voltage. This result verifies the diode voltage stress equation in Table 1. The capacitors' voltages and currents' waveforms are shown in Figure 11.

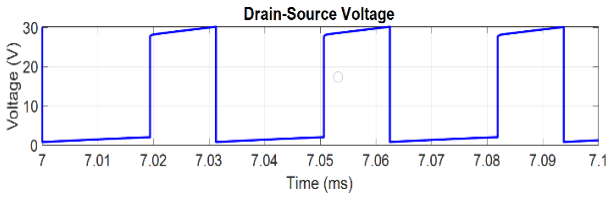

(a)

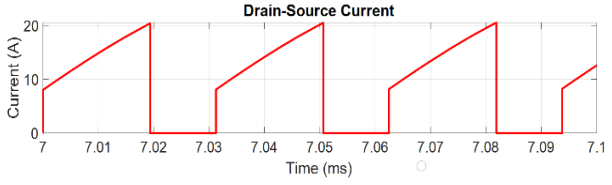

(b)

Fig. 8. The switch's voltage and current, a) drain-source voltage and b) drain-source current.

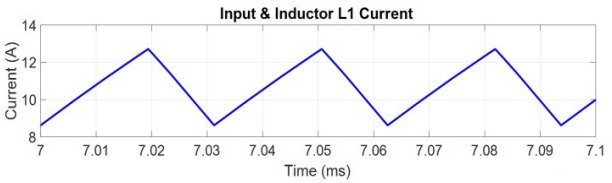

(a)

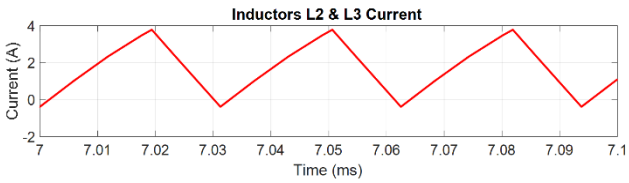

(b)

Fig.9. Inductors' current waveforms, a) L_1 (Input current) and b) L_2 and L_3.

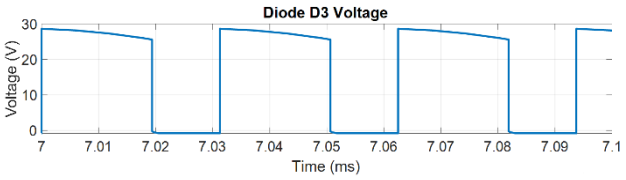

(e)

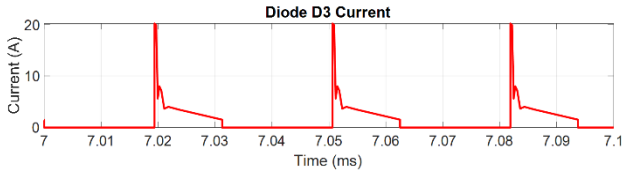

(f)

Fig. 10. Reversed voltage and current waveforms of the diodes, a) D_1 voltage, b) D_1 current, c) D_2 voltage, d) D_2 current, e) D_3 voltage, and f) D_3 current.

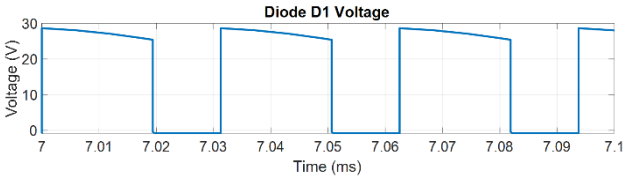

(a)

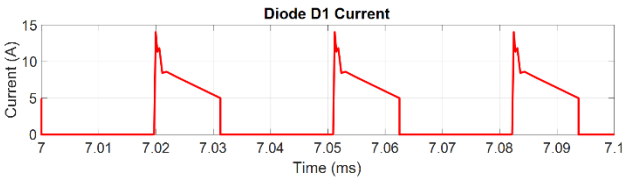

(b)

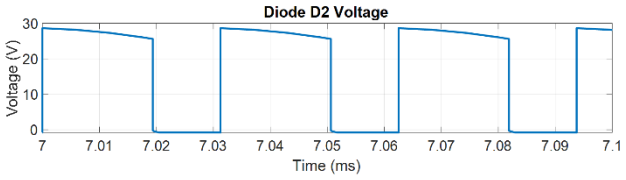

(c)

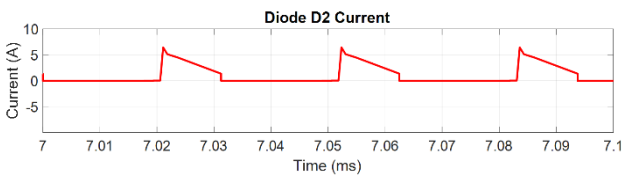

(d)

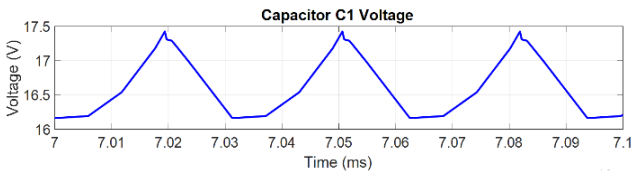

(a)

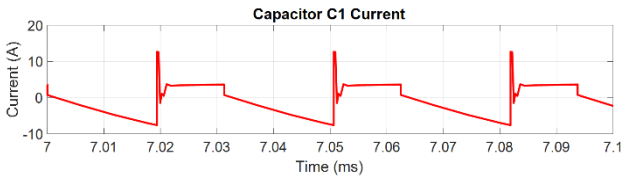

(b)

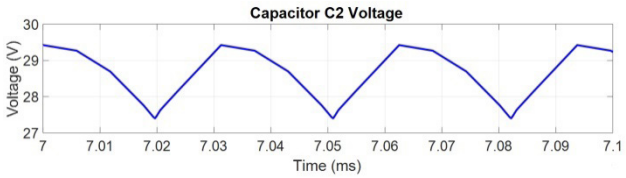

(c)

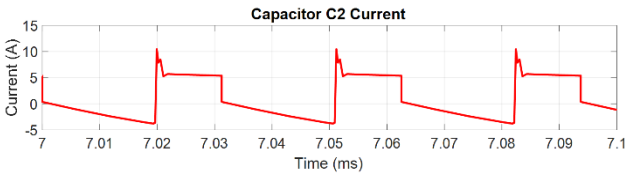

(d)

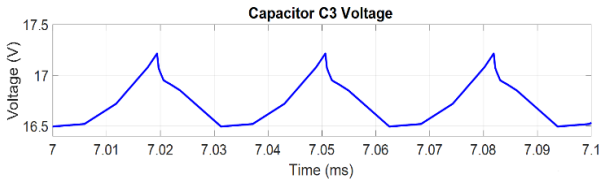

(e)

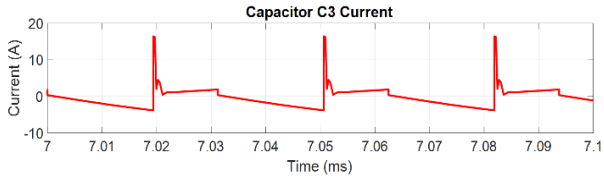

(f)

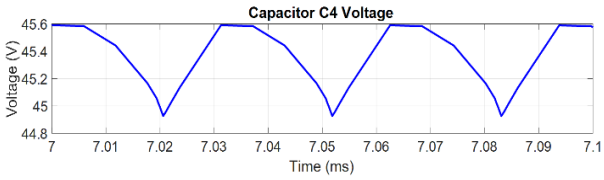

(g)

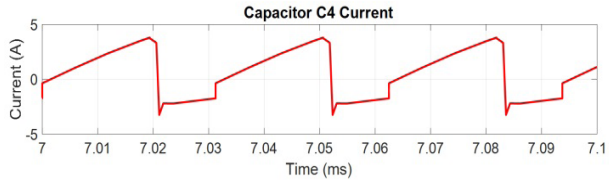

(h)

Fig. 11. Voltage and current waveforms of capacitors, a) C_1 voltage, b) C_1 current, c) C_2 voltage, d) C_2 current, e) Capacitor C_3 voltage, f) Capacitor C_3 current, g) Capacitor C_4 voltage, and h) C_4 current.

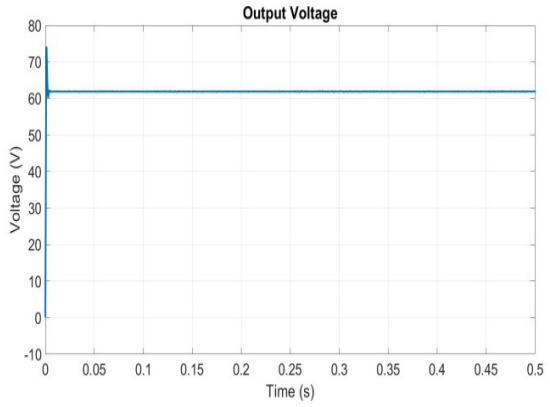

(a)

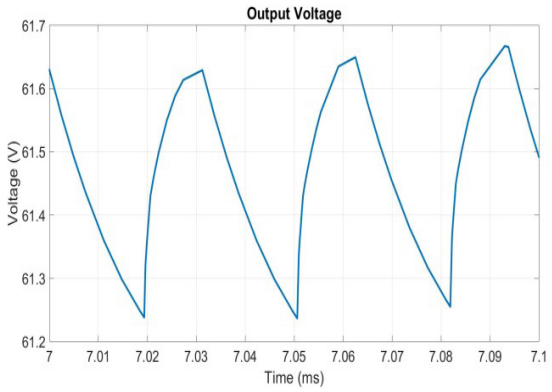

(b)

Fig. 12. The output voltage waveform of the proposed converter, a) 0.5 second duration and b) three cycles duration.

It can be seen that the output voltage shows some desirable features, including low voltage ripple (about 0.1%), low rise time response, and low overshoot.

As shown in Figure 12-a, the output voltage is about 61 V, and the converter voltage gain is about 5. This value is lower than the gain value calculated by equation (15) for the same duty cycle. This difference is due to the converter losses investigated in the next section.

8. Converter losses

The proposed converter losses consist of several losses related to inductors, switch, diodes, and capacitors. The losses of these elements can be derived from the equations presented in Table 3. The power loss calculations are based on the conduction mode resistance and the effective current passing through the element [26]. The parameters of Table 3 are defined in Table 4.

Table3 . Loss Equations of the Proposed Converter Elements

Loss	Equation
Inductors	$P_L = r_{L1} I_{L1-RMS}^2 + r_{L2} I_{L1-RMS}^2 + r_{L3} I_{L3-RMS}^2$
Switches	$P_{S-Cond} = r_{ds} I_{S-RMS}^2$
Diodes	$P_D = I_{D1} V_{F-D1} + I_{D2} V_{F-D2} + I_{D3} V_{F-D3}$
Capacitors	$P_C = I_{C1-C5-RMS}^2 (r_{C1} + r_{C2} + r_{C3} + r_{C4} + r_{C5})$

The total converter loss can be obtained as follows:

$$P_{Loss} = P_L + P_C + P_{S-Cond} + P_D \quad (30)$$

According to the voltage and current values of the elements, the losses of inductors, switch, diodes, and capacitors in the simulated converter are as follows: P_L=7.03 W, P_C=3.61 W, $P_{S\text{-}Cond}$=3.99 W, P_D=4.37 W, and P_{Loss_total}=19 W.

The pie chart of the different elements losses in the simulated converter is shown in Figure 13.

Table4 . Definition of Loss Parameters

Parameters	Definition
P_L	Inductor loss
P_{S-Cond}	Switch conduction loss
P_D	Diode loss
P_C	Capacitor loss
r_L	Inductor internal resistance
I_L	Inductor current
r_{ds}	Drain-Source resistance
I_S	Switch current
I_D	Diode current
V_{F-D}	Diode forward voltage
I_C	Capacitor current
r_C	Capacitor internal resistance

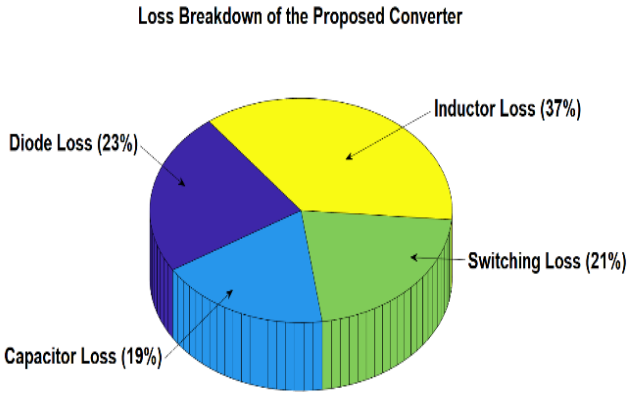

Fig. 13. Loss breakdown of the proposed converter.

According to Figure 13, a significant part of the proposed converter losses is due to the inductors' high current and resistance value.

As mentioned in the previous section, there is a difference between the gain values calculated by the analytical equation and what is derived by the simulation process at 100 W loading level. Equation (15) is derived under ideal conditions, and the internal resistances of the circuit elements are not considered. Also, considering the internal resistances, the voltage gain for different loading levels is not the same. The effects of the internal resistances and loading levels on the analytical voltage gain have been investigated in other studies. For example, the effect of inductor equivalent series resistance value and the load resistance on the voltage gain is investigated in [1], [28, 29], and the real voltage gain is compared with the ideal one.

9. Converter efficiency

Regarding the proposed converter efficiency, it should be noted that as the converter power level decreases to medium or low power levels, the power losses related to the circuit elements take higher portions of the con-

verter's total power, and therefore the efficiency decreases. Since the proposed converter was developed for a medium-power fuel cell system in the range of 100 W, efficiency values in the 70 to 80 % range are considered good compared with high step-up DC-DC converters in similar power ranges. The input voltage range is another parameter that affects the efficiency values. For the same power level, the efficiency increases with the input voltage increment.

The proposed converter efficiency changes is presented for the different voltage levels in the range of 8 to 16 V and at the 100 W loading level, see Figure 14.

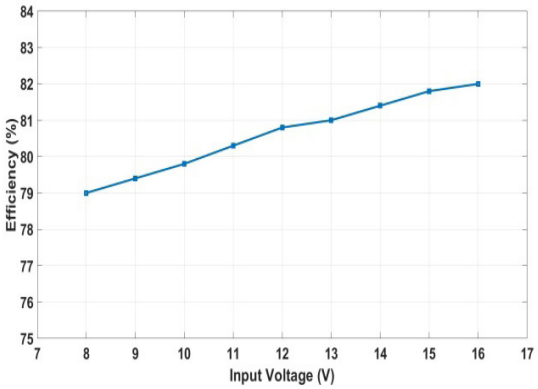

Fig. 14. Efficiency versus input voltage at 100 W loading level.

As can be seen in Figure 14, the converter efficiency at the selected operating point (input voltage=12 V) is about 81%, which is considered a good value in comparison with high step-up DC-DC converters in similar power and voltage ranges.

10. Experimental results

A laboratory prototype of the proposed converter was implemented to validate the theoretical analysis and simulation results. The circuit elements of the implemented converter have similar values to the simulation model and are given in Table 2. The power MOSFET used is IRF540, and the diodes are MUR640. The converter was implemented as a power conditioning module for a Horizon H-100 fuel cell stack to supply a 60 V DC load. Like the simulation process, the loading level of the implemented converter was designed so that the fuel cell stack voltage becomes about 12 V. As seen in Figure 7-b, the stack power, or the converter input power, is about 100 W. The switching frequency is 32 kHz, and the duty cycle is 63%. The switch driver was designed and implemented by NE555.

The experimental test setup is shown in Figure 15. A 12 V lead-acid battery was used to simulate the Horizon H-100 fuel cell stack at the defined operating voltage point.

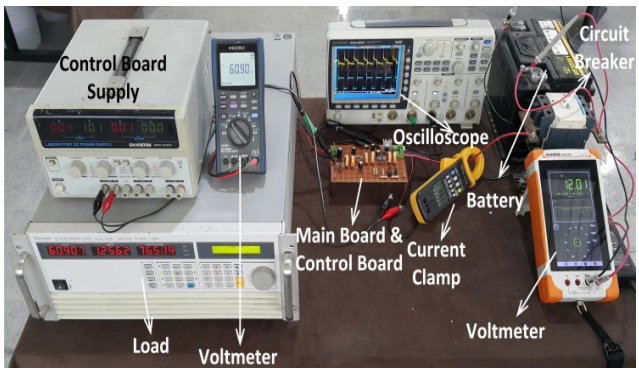

Fig. 15. Experimental test setup for the proposed converter.

The test results are shown in Figure 16. The gate-source and drain-source voltage waveforms are shown in Figures 16-a and 16-b, respectively. The drain-source voltage in Figure 16-b verifies equation (16) and Figure 8-a. Figure 16-c shows the input current waveforms. The RMS value of the input current is 8.5 A when the duty cycle is near 0.63. This value confirms equation (21) and Figure 9-a. Figure 16-d shows the capacitor C_2 voltage; this capacitor acts like the conventional boost capacitor in the first section of the proposed converter (considering Figure 2). The output voltage waveform is shown in Figure 16-e.

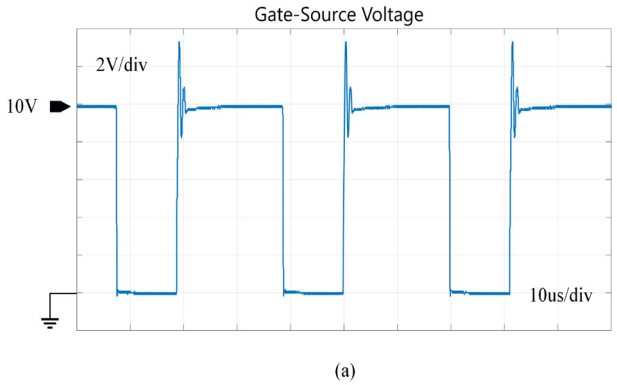

(a)

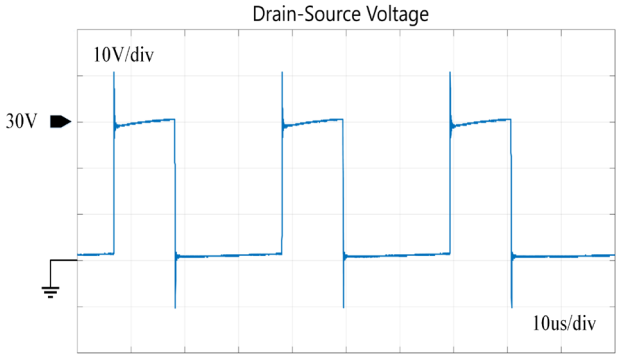

(b)

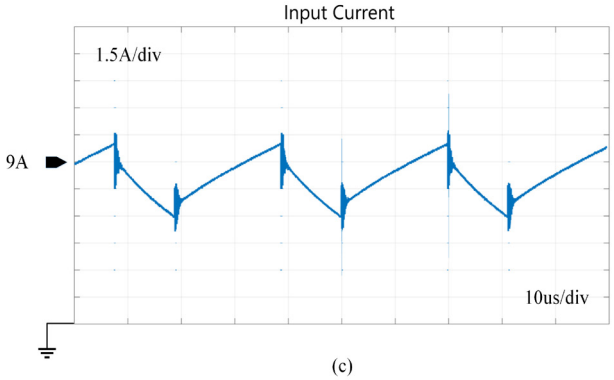

(c)

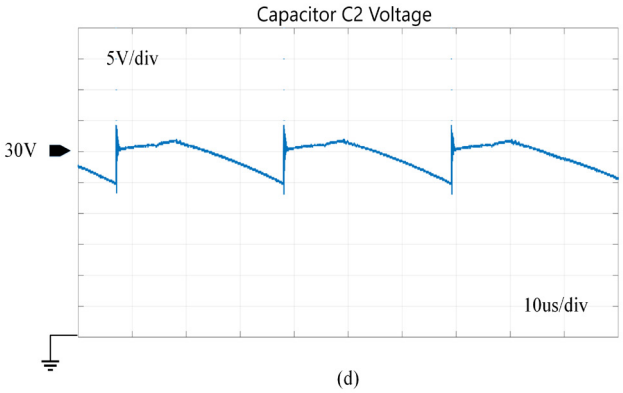

(d)

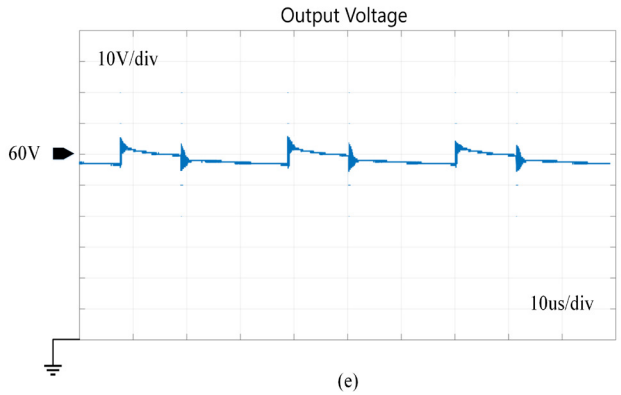

(e)

Fig. 16. a) Gate-source voltage, b) Drain-source voltage, c) Input current, d) Capacitor C_2 Voltage, and e) Output voltage.

The efficiency of the implemented converter was 75%, which can be considered a good efficiency compared to other high step-up DC-DC converters in similar power ranges. The output voltage RMS value is about 61 V. This value verifies the simulated waveform presented in Figure 12. Therefore, the experimental results validate the analytical and simulation results.

11. Conclusion

This paper presents a high voltage gain DC-DC converter topology for fuel cell system applications and its analytical equations. The proposed converter performance parameters are analysed and compared to other conventional and high-voltage gain converters. The results confirm the proposed converter's superiority in features, including voltage gain and voltage stress on the switch for the duty cycles in a range of 0.6 and higher, a common duty cycle range for high gain converters. The performance analysis of the proposed converter for fuel cell applications at 100 Watts loading level was done in the MATLAB/Simulink software environment, and the simulation results were presented and analysed. The operating voltage point and the loading level of the converter were de-

termined according to Horizon H-100 fuel cell stack performance characteristics. Experimental investigation of the analytical and simulation results was done by implementing a 100 W laboratory prototype of the proposed converter. The results validated the converter performance in terms of voltage gain and switch voltage stress. Also, the converter efficiency was measured 75%, which can be considered a good value among the high step-up DC-DC converters with similar power ranges.

References

[1] Bi, H., Wang, P., & Che, Y. (2018). A Capacitor Clamped H-type Boost DC-DC Converter with Wide Voltage-Gain Range for Fuel Cell Vehicles. *IEEE Trans. Vehicular Technology. 68,* (1), 276-290. https://doi.org/ 10.1109/TVT.2018.2884890

[2] Zhu, B., Wang, H., Vilathgamuwa, D.M. (2019). Single-switch high step-up boost converter based on a novel voltage multiplier. *IET Power Electron. 12*, (14), 3732-3738. https://doi.org/ iet-pel.2019.0567

[3]Taghizadeh, K. M., Aleyasin, S. H., Safaeinasab, & A., Abbaszadeh, K. (2021). A New Non-Isolated Single Switch High Step-up DC/DC Converter Based on Inductor Cells. *12th International Power Electronics, Drive Systems and Technologies Conference (PEDStC)* (pp 1-5). Tabriz. Iran.

[4] Wu, B., Li, S., Liu, Y., & Smedley, K.M. (2015). A New Hybrid Boosting Converter for Renewable Energy Applications. *IEEE Tran. Power Electronic. 31*, (2), 1203-1215. https://doi.org/10.1109/TPEL.2015.2420994

[5] Saikripa, M., Dharshini, B.A., Vignesh, B.S., & Annapoorani, K.I. (2019). Design of boost converter with voltage multiplier cell for single phase AC load applications. *ICEES Fifth International Conference on Electrical Energy Systems* (pp 1-6). Chennai. India.

[6] Porselvi, T., & Arounassalame, M. (2018). A novel Single Switch High Gain dc-dc Converter. *8th IEEE India International Conference on Power Electronics (IICPE).* (pp 1-6). Jaipur. India.

[7] Suryoatmojo, H., Mardiyanto, R., Riawan, D.C., Anam, S., & Setijadi, E. (2018). Implementation of High Voltage Gain DC-DC Boost Converter for Fuel Cell Application. *International Conference on Engineering, Applied Sciences, and Technology (ICEASt).* (pp 1-4). Phuket. Thailand.

[8] Pires, V.F., Cordeiro, A., Foito, D., & Silva, J.F. (2019). High Step-Up DC-DC Converter for Fuel Cell Vehicles Based on Merged Quadratic Boost–Cuk. *IEEE Trans. Vehicular Technology. 68,* (8), 7521-7530. https://doi.org/10.1109/TVT.2019.2921851

[9] Zhang,Y., Liu, H., Li, J., Sumner, M., & Xia, C. (2019). A DC-DC Boost Converter with a Wide Input Range and High Voltage Gain for Fuel Cell Vehicles. *IEEE Trans. Power Electron. 34,* (5), 4100-4111. https://doi.org/10.1109/TPEL.2018.2858443

[10] Karthikeyan, V., Vipin, P.D., & Blaabjerg, F. (2018). Implementation of MPPT Control in Fuel Cell Fed High Step up Ratio DC-DC Converter. *2nd IEEE International conference on power Electronics, Intelligent Control and Energy systems.* (pp 1-5), Delhi. India.

[11] Rajaei, A., Khazan, R., Mahmoudian, M., Mar-

daneh, M., & Gitizadeh, M. (2018). A Dual Inductor High Step-up DC/DC Converter Based on the Cockcroft-Walton Multiplier. *IEEE Trans. Power Electronic. 33,* (11), 9699-9709. https://doi.org/10.1109/TPEL.2018.2792004

[12] Elsayad, N., Moradisizkoohi, H., & Mohammed, O. (2019). A Single-Switch Transformerless DC-DC Converter with Universal Input Voltage for Fuel Cell Vehicles: Analysis and Design. *IEEE Trans. Vehicular Technology. 68,* (5), 4537 – 4549. https://doi.org/10.1109/TVT.2019.2905583

[13] Tseng, K.C., & Huang, C.C. (2014). High Step-Up, High Efficiency Interleaved Converter with Voltage Multiplier Module for Renewable Energy System. *IEEE Trans. Industrial Electronics. 61,* (3), 1311-1319. https://doi.org/10.1109/TIE.2013.2261036

[14] Eskandari, R., Babaei, E., Sabahi, M., & Ojaghkandi, S.R. (2016). Interleaved high step-up zero-voltage zero-current switching boost DC–DC converter. *IET Power Electronics. 13*, (1), 96-103. https://doi.org/10.1049/iet-pel.2019.0134

[15] Tang, Q., Li, B., Czarkowski, D., & Ioinovici, A. (2011). Switched-Capacitor Based Step-up Converter for Alternative Energy Applications. *IEEE International Symposium of Circuits and Systems (ISCAS)*. (pp. 1355-1358). Rio de Janeiro. Brazil.

[16] Liu, X., Zhang, X., Hu, X., Chen, H., Chen, L., & Zhang, Y. (2019). Interleaved High Step-Up Converter With Coupled Inductor and Voltage Multiplier for Renewable Energy System. *CPSS Trans. Power Electronic and Applications. 4,* (4), 299-309. https://doi.org/10.24295/CPSSt-PEA.2019.00028

[17] Lin, G., & Zhang, Z. (2019). Low Input Ripple High Step-Up Extendable Hybrid DC-DC Converter. *IEEE Access. 7*, 158744-158752. https://doi.org/10.1109/ACCESS.2019.2950524

[18] Wu, G., Ruan, X., & Ye, Z. (2014). Non-Isolated High Step-Up DC-DC Converters Adopting Switched-Capacitor Cell. *IEEE Trans. Industrial Electronic. 62,* (1), 383-393. https://doi.org/10.1109/TIE.2014.2327000

[19] Chauhan, A.K., Raghuram, M., Tripathi, A.K., Singh, S.K., & Xiong, X. (2018). A High Gain DC-DC Converter based on Switched Capacitor/ Switched Inductor Arrangement. *IEEE International Conference on Power Electronics, Drives and Energy Systems*, (pp. 1-6). Chennai. India.

[20] Shouxiang,L., Zhenning, L., Shang, W., Zheng, Sh., & Jia, P. (2020). A Family of Hybrid Step-up DC-DC Converters based on Switched-capacitor Converters. *IEEE 9th International Power Electronics and Motion Control Conference (IPEMC-ECCE Asia)*. (pp. 1-6). Nanjing. China.

[21] Wang, P., Zhou, L., Zhang, Y., Li, J., Sumner, M. (2017). Input-parallel Output-series DC-DC Boost Converter with a Wide Input Voltage Range, for Fuel Cell Vehicles. *IEEE Trans. Vehicular Technology. 66,* (9), 7771-7781. https://doi.org/10.1109/TVT.2017.2688324

[22] Shahir, F.M., Babaei, E., & Farsadi, M. (2019). Extended Topology for Boost DC-DC Converter. *IEEE Trans. Power Electronic. 34,* (3), 2375-2384. https://doi.org/10.1109/TPEL.2018.2840683

[23] Sedaghati, F., Azizkandi, M.E., Majareh, S.H.L., & Shayeghi, H. (2019). A High-Efficiency Non-Isolated High-Gain Interleaved DC-DC Converter with Reduced Voltage Stress on Devices. *2019 10th International Power Electronics, Drive Systems and Technologies Conference (PEDStC)*.

(pp. 1-6). Shiraz. Iran.

[24] Yazdani, M.R., & Fattahi, S. (2014). An Interleaved High Step-up Switched-Capacitor Converter. *The 5th Annual International Power Electronics, Drive Systems and Technologies Conference (PEDStC 2014)*. (pp. 1-6). Tehran. Iran.

[25] Amudhavalli, D., Mohanty, N.K., & Sahoo, A.K. (2018). High Power High Gain Non-Isolated Interleaved Quadratic Boost Converter with Voltage Multiplier Cell. *Technologies for Smart-City Energy Security and Power (ICSESP)*. (pp. 1-6). Bhubaneswar. India.

[26] Zheng, Y., Xie, W., & Smedley, K.M. (2019). Interleaved High Step-Up Converter with Coupled Inductors. *IEEE Trans. Power Electronic, 34* (7), 6478-6488. https://doi.org/10.1109/TPEL.2018.2874189

[27] H-100 Fuel Cell Stack User Manual. (2014). https://www.fuelcellstore.com/manuals/horizon-pem-fuel-cell-h-100-manual.pdf

[28] Ahmad, J., Lin, Ch. H., Zaid, M., Sarwar, A., Ahmad, Sh., Sharaf, M., Zaindin, M., & Firdausi, M. (2020). A New High Voltage Gain DC to DC Converter with Low Voltage Stress for Energy Storage System Application. *MDPI Electronics Journal. 9* (12), 1-19. https://doi.org/10.3390/electronics9122067

[29] Agrawal, Sh., Atmanandmaya., Reddy, S., Umanand, B, L. (2020). Integration of Photovoltaic Panels with DC Grid Using High Gain DC-DC Converter. *IEEE International Conference on Electronics, Computing and Communication Technologies (CONECCT)*. (pp. 1-6). Bangalore. India.